

Fig. 1—Circuit for line width measurement

in a shorted  $X$ -band waveguide. A nearby pickup coil, which senses the precessing dipolar field of the magnetic sample, is oriented so that the plane of the loop and  $h$  are parallel, producing a negligible coupling to the transverse microwave field. When  $H$  is near resonance a voltage is induced in the loop. Since  $h$  is kept sufficiently small to insure linearity, this voltage is proportional to  $h$ .

The definition of line width depends on the type of response of  $m$  to  $h$  as dictated by the geometry of the system. In general, assuming  $h_x = h_0 e^{i\omega t}$ ,  $h_y = -j h_0 e^{i\omega t}$ ,  $h_z = 0$ ,  $m = (x) \cdot h$  where the elements of the antisymmetric dyadic are complex, substitution yields the circular precession

$$m_x m_x^* = m_y m_y^* = h_0^2 \{ |x_{xx}|^2 + |x_{xy}|^2 + j x_{xx} x_{xy}^* - j x_{xy} x_{xx}^* \}.$$

However, in the use of linear polarization ( $h_x = h_0 e^{i\omega t}$ ,  $h_y = h_z = 0$ ) employed here, there results:

$$m_x m_x^* = h_0^2 |x_{xx}|^2 \quad m_y m_y^* = h_0^2 |x_{xy}|^2.$$

Now the spacial relationship of the loop and sample is such that only the projection of the motion along the  $y$  direction is effective. Therefore, the induced voltage depends upon the absolute value of the off-diagonal component of  $(x)$ , i.e.,  $E \propto h_0 \sqrt{|x_{xy}|^2}$  which may be expressed in terms of its absorptive component,  $x_{xy}$ , whereby the line width may be defined. In general  $|x|^2 = x'^2 + x''^2$  where we have dropped the  $xy$  subscript for convenience. In particular,

$|x|^2 \Delta H \cong [x'_{\max}/2]^2 + [x''_{\max}]^2 \cong 2[x'_{\max}/2]^2$  when  $H$  is set for  $\frac{1}{2}$  of the peak of the absorption curve.<sup>4</sup> Also  $|x|_{\max}^2 = x_{\max}^2$ . The indicated approximations are very good for narrow line width samples yielding

$$|x_{xy}|_{\Delta H} = |x_{xy}|_{\max}/\sqrt{2}.$$

However, since the measurement of the response is normally read from a calibrated attenuator, the observed response as  $H$  varies is of the form  $h_0^2 |x_{xy}|^2$ , and the line width is therefore measured at 3 db below the peak of the response curve.

A simple circuit assembled for these measurements is shown schematically in Fig. 1. The CW source is a Stalo, L. F. E. 814  $\times$  21, operated at 9600 Mc and internally modulated at 1 kc. The sensitivity

gained by modulation allows the use of signals as small as the order to 1 mœ to avoid any saturation or heating effects. The signal is fed through an isolator and calibrated attenuator to a test section terminated in a sliding short. The correct position of the sliding short is found by substitution of an electric probe for the loop and adjusting for a null in the electric probe output. The correct loop orientation is then found by rotation of the loop for minimum leakage of the microwave field with  $H=0$ , which is about 30 db below the loop output when  $H$  is adjusted for resonance.

The loop output is demodulated by a tuned crystal detector and the remaining 1 kc signal is amplified and read on a voltmeter.

Line width measurements are made by noting the field required for resonance and the associated voltmeter readings at attenuator settings of 0 db and 3 db. Twice the difference between the field for resonance and the field required to produce the latter voltmeter reading with the attenuator set at 0 db is the measured line width. Measurements of  $\Delta H$  were made in this experiment by producing field increments with an accurately measured dc current passed through a coil of some 50 turns wound around the yoke of a 6-inch Varian magnet. An  $H$  vs current curve was established using a precision NMR gaussmeter and is a straight line for the current range in question. It has been found that the accuracy ( $\pm 0.01$  gauss) and ease of this method of measuring changes in  $H$  exceeds the method of direct measurements of  $H$  with the gaussmeter.

As anticipated, the distance between the loop and sample is an important consideration. The sample is cemented to a quartz post which may be extracted and rotated by known amounts. In a previous paper,<sup>5</sup> it has been shown that currents in the loop will produce fields that will damp the motion of the resonant sample. Although the formulas of this paper appear not to apply here because of the uncertainty in the phase relationship between loop voltage and current, decoupling of the sample and loop by increasing their spacing will reduce the damping. The sample is thus extracted as far from the loop as possible without reducing the signal-to-leakage ratio in the loop output below an arbitrary figure of 30 db. For two single crystal YIG sphere samples tested, a spacing of greater than 5-sphere diameters was used. The results of a comparison between the cavity perturbation method and the loop method are given below:

Sample	Diameter in Inches	X-Band Cavity	X-Band Loop Method
A	0.015	0.63 oe	0.65 oe
B	0.020	0.64 oe	0.67 oe

Sample A was grown in the Air Force Cambridge Research Center and polished by a novel manual process to be described in a later letter. Sample B was purchased as a polished sphere from Microwave Chemicals,

Inc., New York, N. Y. The dependence of line width on crystal orientation was eliminated from the comparison by averaging over many orientations in each case.

J. I. MASTERS  
Technical Operations, Inc.  
Burlington, Mass.  
B. R. CAPONE  
P. D. GIANINO  
AF Cambridge Res. Center  
Air. Res. and Dev. Command  
Laurence G. Hanscom Field  
Bedford, Mass.

## Multidiode Switches\*

The impedance of crystal diodes is known to depend on the applied bias voltage. This has suggested the use of diodes as switching elements in the control of microwave signal transmission. In the simplest form, the diode switch consists of a transmission line which is shunted by a diode. Coaxial cables<sup>1</sup> as well as waveguides<sup>2-5</sup> have been used for the transmission lines that are shunted by point-contact<sup>1-5</sup> and *p-i-n* diodes.<sup>6</sup> Slab line or coaxial switches where a diode is inserted in series with the center conductor of the line have also been developed.<sup>7</sup>

This note examines the feasibility of multidiode shunt or series type switches. After establishing equivalent circuits representative of the diodes in the "on" and "off" states of the switch, a specific realizable single diode switch is assumed for the calculations. Characteristics of a multipole switch which consists of a number of diodes in individual transmission line branches are derived for the two switch types. Several measurements made on an 8-diode series switch will be described thereafter.

### SHUNT-TYPE DIODE SWITCHES

The diode switch configuration consisting of a diode which shunts a transmission line will be considered first for multidiode

\* Received by the PGMTT, April 18, 1960; revised manuscript received, May 26, 1960. This note is based on a presentation at the 1959 National Symposium of the Professional Group on Microwave Theory and Techniques, Harvard University, Cambridge, Mass.

<sup>1</sup> D. J. Grace, "A Microwave Switch Employing Germanium Diodes," Appl. Elec. Lab., Stanford University, Stanford, Calif. Tech. Rept. No. 26; January, 1955.

<sup>2</sup> M. A. Armstead, E. G. Spencer, and R. D. Matcher, "Microwave semiconductor switch," PROC. IRE, vol. 44, p. 1875; December, 1956.

<sup>3</sup> R. V. Garver, E. G. Spencer, and M. A. Harper, "Microwave semiconductor switching techniques," IRE TRANS. ON MICROWAVE THEORY AND TECHNIQUES, vol. MTT-6 pp. 378-383, October, 1958.

<sup>4</sup> M. R. Millet, "Microwave switching by crystal diodes," IRE TRANS. ON MICROWAVE THEORY AND TECHNIQUES, vol. MTT-6, pp. 284-290; July, 1958.

<sup>5</sup> M. Depoy and R. Lucy, "An Absorption Type Microwave Crystal Switch for High Speed Duplexing," Sylvania Electric Products, Inc., Waltham, Mass., Appl. Res. Memo. No. 140; July, 1958; also R. Lucy, "Microwave High Speed Switch," Proc. 1959 Electronic Components Conf., Philadelphia, Pa., May 6-8, 1959; pp. 12-25.

<sup>6</sup> A. Uhli, Jr., "The potential of semiconductor diodes in high-frequency communications," PROC. IRE, vol. 46, pp. 1099-1115; June, 1959. (See especially pp. 1112-1113.)

<sup>7</sup> M. Bloom, "Single-Pole Double-Throw Wide-Band Microwave Switch," National Symposium of the Professional Group on Microwave Theory and Techniques, Harvard University, Cambridge, Mass.; 1959.

<sup>4</sup> A relationship between absorption and dispersion that approximately satisfies the Kramers-Kronig formula is assumed.

<sup>5</sup> N. Bloembergen and R. V. Pound, "Radiation damping in magnetic resonance experiments," Phys. Rev., vol. 95, pp. 8-12; July, 1954.

TABLE I\*  
PERFORMANCE OF SINGLE POLE SHUNT TYPE DIODE SWITCHES

		Armstead, et al. <sup>2</sup>	Millet <sup>3</sup>	Depoy and Lucy <sup>4</sup>	Sylvania <sup>8</sup>	Assumed Switch Characteristics
Incident Power, Milliwatts		0.1	0.5	0.1	1000 to 4000	
"on" Condition	Admittance, Normal	$0.95 - j0.15$	$1.25 - j0.05$	$1.25 - j0.03$	—	$1.25 - jb$
	Insertion Loss, db	1	1	1	0.5	1
"off" Condition	Admittance, Normal	$18 + j15$	8	$2.2 - j3.4$	—	$y_{off}$
	Reflected Power, Per cent	80	60	60	90	80
Insertion Loss, db		25	21	22	25 to 19	$k$

\* The listed admittance figures include the admittance of a matched line termination.

switch applications. The data published by several authors<sup>2,4,5</sup> and recent experimental data of Sylvania<sup>8</sup> are summarized in Table I. The characteristics of the switch assumed for the subsequent analysis are indicated in the last column of the Table. The admittance of the "off" diodes should be commensurate with the 80 per cent power reflection figure, but is not further specified.

The equivalent circuit of a single pole diode switch to be used in a multipole switch synthesis must account for the experimental data of Table I. Although equivalent two-terminal network representations have been suggested for the switch during its "on" and "off" conditions,<sup>4</sup> such networks characterize the switch performance only qualitatively. The loading of the transmission line by the diode admittance may account for the insertion loss observed in most cases during the "on" condition, but one must resort to a four-terminal structure to represent the observed insertion loss during the "off" condition of the switch. The "on" condition of the switch is represented by an admittance  $Y_d$  which shunts the transmission line. The normalized diode admittance

$$y_d = \frac{Y_d}{Y_0} = 0.25 - jb \quad (1)$$

when added to the matched line admittance  $y_0 = 1$  provides the insertion loss listed in two cases<sup>4,5</sup> of Table I. With a standing wave ratio of approximately 1.2, the reflection loss is less than 0.1 db. Power division between the diode and the matched load provides the measured insertion loss of approximately 1 db. In the "off" condition, the equivalent shunt admittance provides the correct amount of reflected power, but it gives too small an insertion loss in all of the cases listed in Table I. Thus, 60 per cent of reflected power corresponds to a reflection coefficient  $|\Gamma| = 0.775$  and to the normalized input admittances  $y_s = 8$  or  $2.2 - j3.4$  as listed in the Table.<sup>4,5</sup> The smallest amount of power is delivered to the load  $Y_0$  if the real part of  $Y_d$  has its maximum value which is the case for real  $Y_d$ . With  $y_s = 8$  the power division between  $Y_0$  and  $Y_d$  is 1:7. The power delivered to the load  $Y_0$  is thus  $0.4:7 \approx 0.057$  of the incident power; the in-

sertion loss is no greater than 12.5 db which is almost 10 db short of the measured insertion loss. The insertion loss measured in the "off" condition can be accounted for by a four-terminal equivalent network. A  $T$ -type structure has been selected for the equivalent representations of multidiode switches.

A multidiode switch may be designed to connect a centrally located source to one of  $n$  possible loads. Such a switching device is designated as a distribution switch. Its equivalent diagram is shown in Fig. 1. The isolation and insertion losses of this switch have been calculated for the diode characteristics indicated in the last column of Table I. The total insertion loss relative to the load at the "on" diode ( $L_{on}$ ) consists of the reflection loss due to the mismatch of the central junction as seen from the incident wave, a power division loss between the  $(n-1)$  "off" diodes and the "on" diode and of a further power division loss between the "on" diode and the load. The total insertion loss relative to the load at the "off" diode ( $L_{off}$ ) consists of the reflection loss from the central junction, a power division loss between the "off" diode on one side and the "on" diode and the  $(n-2)$  "off" diodes on the other side, the nominal isolation ( $k$ ) provided by a single "off" diode less the single "off" diode reflection loss (7 db for 80 per cent reflected power), since the latter part of the single diode isolation is accounted in the earlier power division losses. In designing the multidiode switch, the line length  $l$  between the central junction and the individual diodes is selected in such a way that the "off" diodes reflect minimum conductance across the central junction. This choice of line length minimizes the part of insertion losses  $L_{on}$  caused by power division between the load and the "off" switches. As seen in Table I, the "off" switches exhibit a high input admittance. Therefore, the line length  $l$  will be very nearly an odd multiple of  $(\lambda/4)$ . For a purely conductive input admittance of the "off" switches

$$l = (2m + 1)(\lambda/4) \quad (2)$$

where  $m$  is an integer or zero. The loss figures computed for this line length are indicated by solid curves in Fig. 2. For a complex input admittance of the "off" switches, the loss figures will lie within the shaded areas, close to the solid curves. The shaded areas are bounded by dashed curves that represent loss figures in the hypothetical case of  $l$ , a multiple of  $\lambda/2$  for "off" switches of low

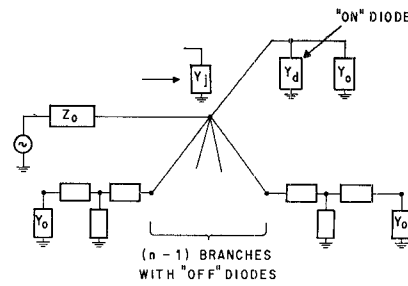


Fig. 1—Multidiode distribution switch.

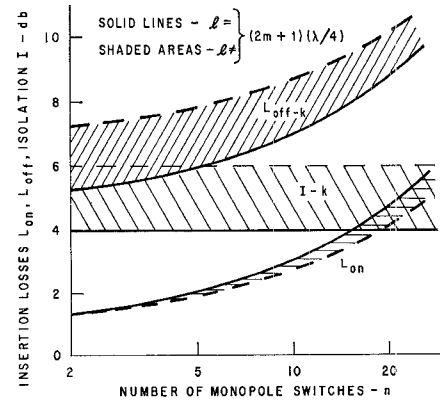
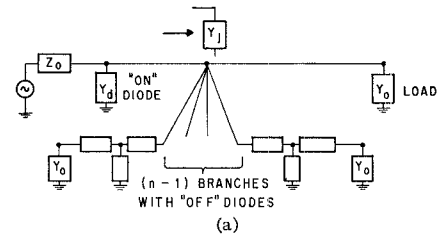
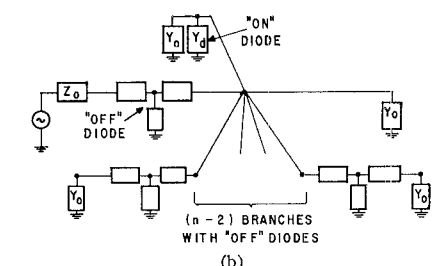


Fig. 2—Insertion losses and isolation of a shunt-type multidiode switch. Isolation  $I = L_{off} - L_{on}$ ;  $k$  = "off" insertion loss of a one-diode switch.



(a)



(b)

Fig. 3—Multidiode selector switch; (a) "on" condition (b) "off" condition.

purely conductive input admittance. It is seen that both the losses in the "on" and "off" conditions of the switch increase with an increasing number of diodes  $n$ . However, the isolation provided by the switch remains constant over the range of  $n$  indicated in Fig. 2.

In another switch configuration, a centrally located load may be connected to one of  $n$  possible locations of a single source (as in a scanning receiving antenna). Such a switching device is designated as a selection switch and its equivalent diagram is shown in Fig. 3. The same physical structure may be used for distribution and selection switches. The switches act as linear devices

<sup>8</sup> Unpublished X-band measurements on 1N419 diodes, by the Appl. Res. Lab., Sylvania Electronic Systems, Inc., Waltham, Mass. No switch impedances were recorded in these tests.

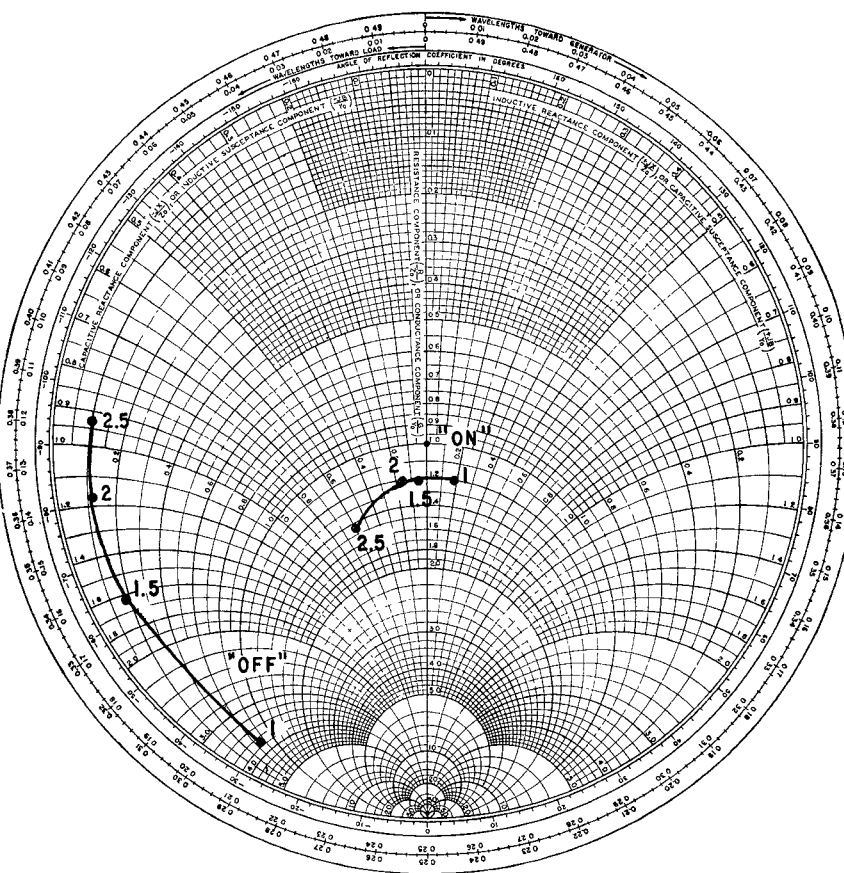


Fig. 4—Input impedance of a series-type diode switch, 50  $\Omega$  line termination, 1N118 diode, frequency in kMc.

during any of their possible states and the reciprocity theorem may be applied to show that the distribution and selection switches exhibit identical loss figures.<sup>9</sup>

#### SERIES-TYPE DIODE SWITCHES

A typical impedance plot of a single diode series type slab line switch is plotted in Fig. 4. The corresponding "on" condition insertion loss is 1 db. The isolation decreases from 29 to 21 db as the frequency is increased from 1 to 2.5 kMc.

The "on" condition of the switch is represented by an impedance in series with the transmission line. The impedance plotted in Fig. 4 provides a reflection loss of less than 0.1 db in the frequency range between 1 and 2.5 kMc. The power division between the diode and the matched load provides the measured insertion loss of approximately 1 db. The two-terminal equivalent representation does not provide the measured insertion loss in the "off" condition. Again a four-terminal structure may be used to characterize the "off" condition.

The equivalent representation of a series type multidiode switch is of the form indicated in Figs. 1 and 3 except for the "on" diode equivalent circuits. The shunt type "on" diodes should be changed to series type "on" diodes in the diagrams of Figs. 1 and 3. The computation of the loss figures of

the multidiode series switch follows closely the pattern of shunt diode computations. However, a significant distinction between the two switch types is their "off" impedance. The series type "off" diodes exhibit high impedance as seen from Fig. 4. In order to minimize the insertion losses caused by power division between the load and the "off" diodes, the line length  $l$  between the central junction and the "off" diodes must be an approximate multiple of  $(\lambda/2)$ . For a purely resistive impedance of the "off" diodes,

$$l = m\lambda/2 \quad (3)$$

where  $m$  is an integer or zero. The analysis shows that the loss figures of the series type switches are identical with those of the shunt type switches, provided the single diode insertion loss and isolation figures are identical and provided that the "on" diode shunt admittance of the shunt switch is equal to the series impedance of the series switch. Within these limitations, the loss curves indicated in Fig. 2 apply also to the shunt type switch except that the solid curves refer to series switches where the line length  $l$  is given by (3). For different line lengths, the loss figures will be within the shaded areas close to the solid curves.

#### DESIGN CONSIDERATIONS AND MEASUREMENTS

The previous discussion indicates that series and shunt type switches are equally

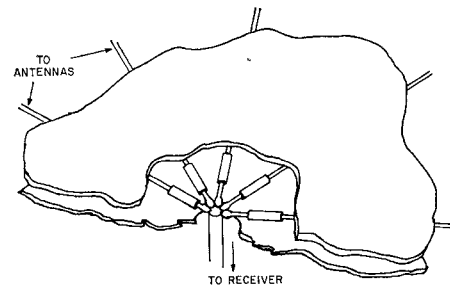


Fig. 5—Diode distribution network.

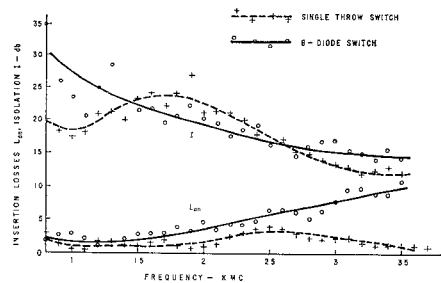


Fig. 6—Measured characteristics of series-type diode switches.

suitied for synthesis of a multidiode switch, provided that their characteristics in single-diode switches are equivalent. The selection between the two switch types may be based on frequency characteristics, bandwidth considerations or fabrication problems.

The operation of series type switches is rapidly deteriorated with increasing operating frequency. This limitation is less pronounced with shunt type switches. A wide operation bandwidth may be achieved only with series type switches. By placing the series diode as close to the central junction as possible, small power division losses may be achieved over a frequency range exceeding an octave [ $m \approx 0$  in (3)]. The shunt diode which exhibits a low "off" impedance must be placed approximately an odd number of quarter wavelengths away from the central junction [ $m$  zero or integer in (2)]. This condition may be satisfied only over small fractional bandwidth to frequency ratios.

A slab line series type switch performs satisfactorily for frequencies up to 3 kMc. Also, the simplicity of its construction makes one favor this switch relative to shunt type switches. As shown in Fig. 5, the switch consists of a central junction and of a number of diodes connected around this junction. Such a switch consisting of 8 diodes has been designed and tested. Preliminary measurement data of Fig. 6 affirm several of the analytical results. The multidiode switch exhibits higher insertion losses, but it provides roughly the same isolation figures as a single-diode switch.

A more recent design of a multidiode switch has resulted in insertion losses that are less than 4 db over the frequency range indicated in Fig. 6.<sup>10</sup>

<sup>9</sup> A long-hand analysis of the selection switch thus provides a cross-check for the loss figure calculations of the distribution switch.

<sup>10</sup> Unpublished measurements on a five-diode switch by J. Kellett of Sylvania's Antenna and Microwave Laboratory.

## ACKNOWLEDGMENT

The experimental work on the 8-diode switch has been carried out under the direction of S. Miller. It was sponsored by USAF Cambridge Research Center.

JANIS GALEJS  
Sylvania Electronic Systems  
Waltham, Mass.

### Technique for Polishing Single Crystal Yttrium-Iron-Garnet Spheres\*

A simple method of polishing yttrium-iron-garnet spheres which produces samples of fractional oersted linewidths has been employed at the Air Force Cambridge Research Center. The technique consists of "hand-polishing" the crystal spheres in diamond pastes and aluminum oxide powders of diminishing grit sizes. This method significantly increases, both by greater pressure and efficiency of abrasive contact, the rate of removing material from the surface

3  $\mu$ -, 1  $\mu$ -, and 0.5  $\mu$ -diamond pastes, followed by dry aluminum oxide powders of grit size 0.3  $\mu$  and 0.1  $\mu$ . Toward the conclusion of the process, the aluminum oxide powder was mixed with acetone into a slurry, yielding an extremely high degree of polish.

At regular intervals within each polishing phase, a visual inspection under a 90X microscope was made and the linewidth of the sample was measured to compare the effectiveness of each grit size in narrowing the linewidth. Table I lists the measured linewidths of three YIG spheres for various grit sizes and polishing times.

Samples A and B were grown in the same batch in the laboratory, while sample C was purchased. Sample B, though adequately polished, appears to have solvent inclusions which probably account for its relatively large linewidth.

Each value listed in the preceding table is the average linewidth taken over many sample orientations, thereby eliminating any dependency of linewidth on crystal orientation. These values were obtained using both the cavity perturbation technique,<sup>2</sup> where appropriate, and a new method<sup>3</sup> designed especially for use with narrow linewidth samples.

TABLE I  
LINEWIDTH IN OERSTEDS

At completion of coarse-polishing phase		Sample A	Sample B	Sample C
Grit Size	Hours	4.47	2.5	~3.0
6 $\mu$ -Diamond Paste	1/2	—	—	1.89
3 $\mu$ -Diamond Paste	1/2	2.72	—	1.39
1 $\mu$ -Diamond Paste	1/2	1.35	1.30	1.13
0.5 $\mu$ -Diamond Paste	1/2	1.27	—	1.16
0.3 $\mu$ -Alumitum Oxide Powder	1/2	1.00	1.25	0.84
0.1 $\mu$ -Aluminum Oxide Powder	1/2	1.05	—	—
	1	1.00	1.24	—
	1/2	0.86	—	0.73
	1	0.95	1.25	—
	2	—	1.04	—
	3	—	1.03	—
Final Diameters	1/2	0.80	—	—
	1	0.65	—	—
	2	—	1.07	—
	3	—	1.12	0.014 inch
		0.015 inch	0.021 inch	

of the sample, which is fundamental in the polishing process. Results attest to a substantial reduction in fine-polishing time to a matter of hours. At present, fine-polishing using the more or less conventional technique of tumbling the sample in an air-cyclone chamber requires a period of days.

Rough samples are shaped into spheres and the coarse-polishing phase completed by either the previously mentioned air-cyclone chamber or metallurgical grinder<sup>1</sup> methods. Fine-polishing is initiated by rolling the spheres in a figure eight pattern under light finger pressure in 6  $\mu$ -grit diamond paste that has been dabbed on a metallurgical polishing cloth. Since a very small amount of material is removed by hand polishing, reasonable care insures uniform polish over the entire crystal surface and maintains sample sphericity. After approximately one hour of such polishing, the process is repeated with successively finer grits, *viz.*,

It is felt that further experience will reveal not only that one or more steps can be eliminated in the polishing procedure, but also that an optimum polishing time per stage can be determined.

To mechanize the process, a simple polishing machine consisting essentially of two reciprocating polishing plates is being developed.

P. D. GIANINO  
B. R. CAPONE  
E. KELLY

AF Cambridge Res. Center  
Air Res. and Dev. Command  
Laurence G. Hanscom Field  
Bedford, Mass.

J. I. MASTERS  
Technical Operations, Inc.  
Burlington, Mass.

<sup>1</sup> J. A. Artman and P. E. Tannenwald, "Microwave Susceptibility Measurements in Ferrites," M.I.T. Lincoln Lab., Lexington, Mass., Tech. Rept. No. 70; October, 1954.

<sup>2</sup> J. Masters, B. Capone, and P. Gianino, "Measurement technique for narrow linewidth ferromagnets," IRE TRANS. ON MICROWAVE THEORY AND TECHNIQUES, this issue, p. 330.

### Tunable Two-Mode Cavity with Capacitative Loading\*

A cavity with two independently tunable modes in the 4- to 9-kMc frequency range was needed for experiments in paramagnetic relaxation. It had to be small enough to fit inside a liquid helium dewar and had to possess a region of approximately uniform RF magnetic field common to both modes over part of its volume.

To meet these requirements a box shaped copper cavity of inside dimensions 0.670 inch  $\times$  0.670 inch  $\times$  0.866 inch was built, and its natural resonant frequencies were lowered into the required range by means of copper blocks mounted in the central region. If the cavity is regarded as the limiting case of an LC resonant circuit, the effect of such loading is to increase the capacity. The fundamental unloaded frequencies were 11.18 kMc in the two modes which were used and 12.48 kMc in the third mode. The 11.18-kMc modes were shifted to frequencies in the range from 4 to 9 kMc by an appropriate choice of loading block. The third mode was damped out by the joint in the cavity wall and by the brass rod used to support the center block. The cavity was tuned by moving dielectric plungers in and out of the region of the strong electric field. In most of the geometries tested, these regions were distinct for each mode so that changes in the tuning of one had comparatively little effect on the other.

The cavity was made in two parts joined along a central plane as shown in Fig. 1.

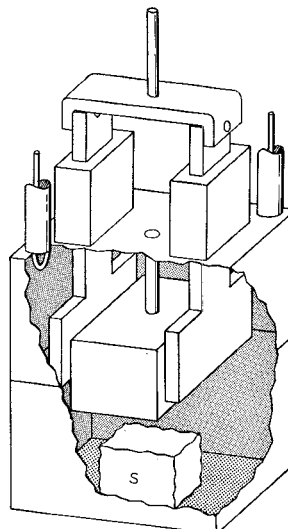


Fig. 1—Cutaway view of loaded cavity. In magnetic resonance experiments the sample (S) may be placed in the space below the loading block. For clarity, only one pair of dielectric tuning plungers are shown.

Dielectric plungers, loading blocks, and coupling loops were mounted in the upper part, the lower part being left for accommodation of the specimen. The plungers were made of SC24 ceramic (relative dielectric constant 9) and connected in pairs by brass brackets outside the cavity so that each

\* Received by the PGMTT, June 1, 1960.

<sup>1</sup> J. L. Carter, E. V. Edwards, and I. Reingold, "Ferrite sphere grinding technique," Rev. Sci. Instr., vol. 30, pp. 946-947; October, 1959.